Escape of SARS-CoV-2 501Y.V2 variants from neutralization by convalescent plasma

Sandile Cele[1,2], Inbal Gazy[2,3,4], Laurelle Jackson[1], Shi-Hsia Hwa[1,5], Houriiyah Tegally[3], Gila Lustig[6], Jennifer Giandhari[3], Sureshnee Pillay[3], Eduan Wilkinson[3], Yeshnee Naidoo[3], Farina Karim[1,2], Yashica Ganga[1], Khadija Khan[1], Alejandro B. Balazs[7], Bernadett I. Gosnell[8], Willem Hanekom[1,5], Mahomed-Yunus S. Moosa[8], NGS-SA[§], COMMIT-KZN Team[§§], Richard J. Lessells[2,3,6], Tulio de Oliveira[2,3,6,9*], Alex Sigal[1,2,10*]

[1]Africa Health Research Institute, Durban 4001, South Africa. [2]School of Laboratory Medicine and Medical Sciences, University of KwaZulu-Natal, Durban 4001, South Africa. [3]KwaZulu-Natal Research Innovation and Sequencing Platform, Durban 4001, South Africa. [4]Department of Biochemistry and Molecular Biology, The Institute for Medical Research Israel-Canada, Hadassah Medical School, The Hebrew University of Jerusalem, 91120, Jerusalem, Israel. [5]Division of Infection and Immunity, University College London, London WC1E 6BT, UK. [6]Centre for the AIDS Programme of Research in South Africa, Durban 4001, South Africa. [7]Ragon Institute of MGH, Harvard, and MIT, Cambridge, USA. [8]Department of Infectious Diseases, Nelson R. Mandela School of Clinical Medicine, University of KwaZulu-Natal, Durban 4001, South Africa. [9]Department of Global Health, University of Washington, Seattle, USA. [10]Max Planck Institute for Infection Biology, Berlin 10117, Germany.

[*] Corresponding authors. Email: deoliveira@ukzn.ac.za, alex.sigal@ahri.org

Abstract

New SARS-CoV-2 variants with mutations in the spike glycoprotein have arisen independently at multiple locations and may have functional significance. The combination of mutations in the 501Y.V2 variant first detected in South Africa include the N501Y, K417N, and E484K mutations in the receptor binding domain (RBD) as well as mutations in the N-terminal domain (NTD). Here we address whether the 501Y.V2 variant could escape the neutralizing antibody response elicited by natural infection with earlier variants. We were the first to outgrow two variants of 501Y.V2 from South Africa, designated 501Y.V2.HV001 and 501Y.V2.HVdF002. We examined the neutralizing effect of convalescent plasma collected from six adults hospitalized with COVID-19 using a microneutralization assay with live (authentic) virus. Whole genome sequencing of the infecting virus of the plasma donors confirmed the absence of the spike mutations which characterize 501Y.V2. We infected with 501Y.V2.HV001 and 501Y.V2.HVdF002 and compared plasma neutralization to first wave virus which contained the D614G mutation but no RBD or NTD mutations. We observed that neutralization of the 501Y.V2 variants was strongly attenuated, with IC_{50} 6 to 200-fold higher relative to first wave virus. The degree of attenuation varied between participants and included a knockout of neutralization activity. This observation indicates that 501Y.V2 may escape the neutralizing antibody response elicited by prior natural infection. It raises a concern of potential reduced protection against re-infection and by vaccines designed to target the spike protein of earlier SARS-CoV-2 variants.

Through genomic surveillance of the severe acute respiratory syndrome-related coronavirus 2 (SARS-CoV-2), a number of new variants have recently been identified with multiple mutations in the spike glycoprotein [1, 2, 3]. We recently described the emergence of the N501Y.V2 variant in South Africa, characterised by the K417N, E484K, and N501Y mutations in the spike receptor binding domain (RBD) as well as four substitutions and a deletion in the N-terminal domain (NTD) [1]. This variant was first detected in October 2020, and has rapidly become the dominant variant in several parts of the country at a time of a rapid resurgence in infections.

The RBD is the main target of neutralizing antibodies (NAbs) elicited by SARS-CoV-2 infection, with the remaining activity directed at the NTD [4, 5, 6]. All three amino acid residues in the RBD that carry mutations in 501Y.V2 interact directly with the human angiotensin-converting enzyme 2 (hACE2) receptor and form part of the epitopes for hACE2-blocking NAbs [7]. The E484 residue specifically is a hotspot for binding of highly potent NAbs [7]. In a number of separate *in vitro* studies using monoclonal antibodies (mAbs), mutations at E484 have emerged as immune escape mutations, often conferring broad cross-resistance to panels of mAbs [8, 9, 10, 11]. E484K also emerged during passage with convalescent plasma, leading to substantial drops in neutralization with convalescent plasma samples [12, 13]. Using a deep mutation scanning approach to determine the effect of individual mutations on neutralization by polyclonal serum, mutations at E484 were associated with the largest drops in neutralization [14].

Here, using a microneutralization assay with authentic virus, we address the question of whether 501Y.V2 variants can escape the neutralizing response elicited by natural infection with previous variants. We outgrew and compared the neutralization of two SARS-CoV-2 501Y.V2 variants to a previously circulating variant derived from South Africa which does not have the 501Y.V2 defining mutations.

For neutralization, we used plasma samples from our ongoing longitudinal cohort study that tracks COVID-19 cases enrolled at two hospitals in Durban, South Africa [15]. We sampled participants weekly for the first month post-enrollment, and at each timepoint a blood draw and combined nasopharyngeal/oropharyngeal swab was performed to obtain both the plasma and the infecting virus.

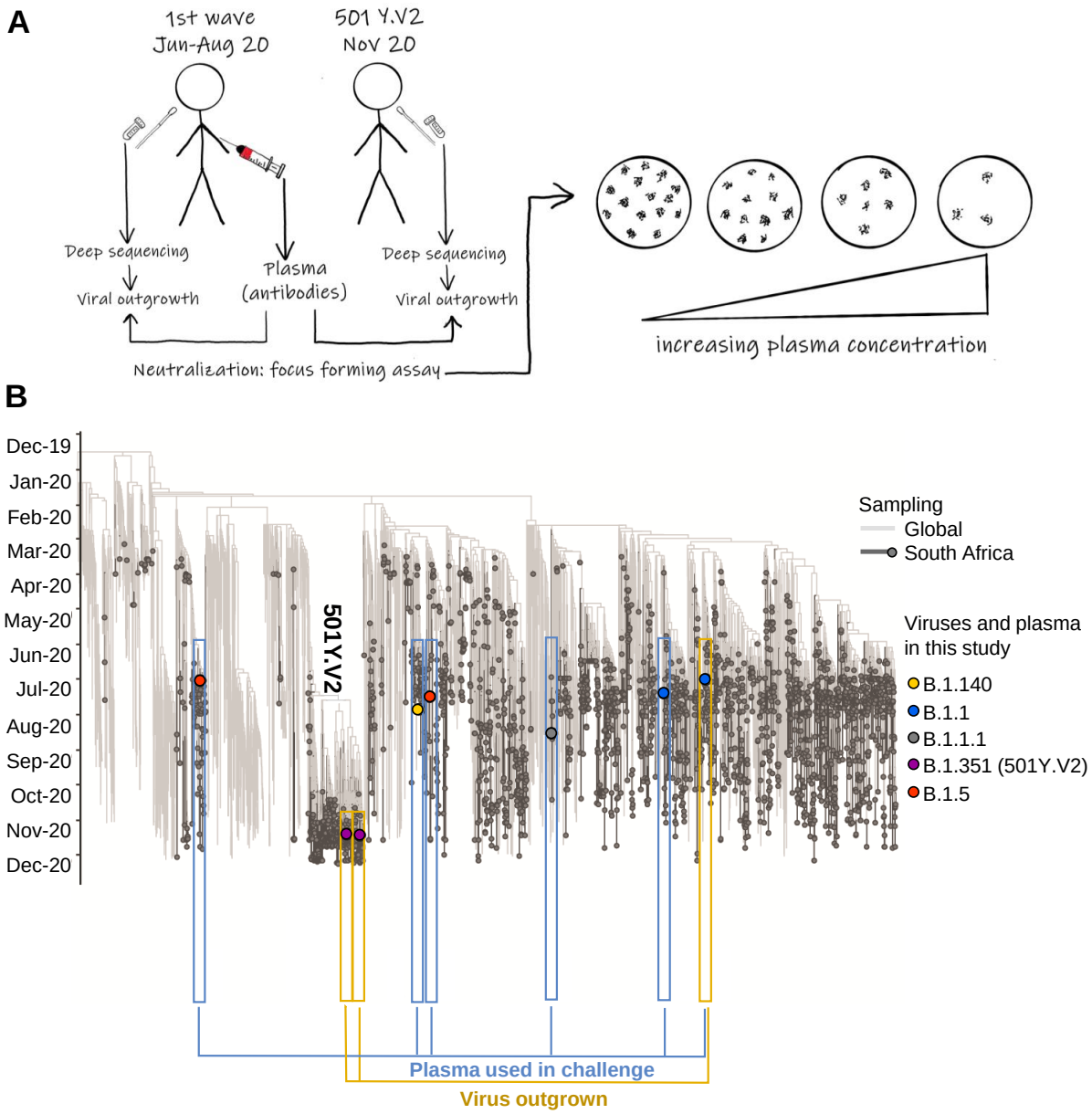

	Outgrown viral variants			Infecting variant sequences of blood plasma donors					
Lineage	B.1.1	501Y.V2 (B.1.351)		B.1.1	B.1.1	B.1.5	B.1.5	B.1.140	B.1.1.1
Sequence ID	K002868	K005321	K005325	K002868	K004289	K004285	K004291	K004295	K004302
Plasma ID	039-13-0013			039-13-0013	039-02-0014	039-13-0015	039-13-0033	039-02-0017	039-13-0062
Isolate designation	CoV2.V003	501Y.V2. HVdF002	501Y.V2. HV001						
Spike mutations	D614G A688V	D80A D215G K417N E484K N501Y D614G A701V	L18F D80A D215G K417N E484K N501Y D614G A701V	D614G A688V	D614G	D614G	D614G	D614G	D614G
Spike indels		242-244del	242-244del						

Figure 1: Study design and sequences of SARS-CoV-2 variants. (A) We obtained convalescent plasma and detected the matching infecting variant in the first SARS-CoV-2 infection wave in South Africa. A blood draw and nasopharyngeal/oropharyngeal was performed on study participants. First wave virus was outgrown from one of the participants and compared to two viruses outgrown from the second wave, which were 501Y.V2 variants. A focus forming microneutralization assay was used to quantify neutralization. (B) Phylogenetic tree and mutations of variant sequences. Variants which infected the study participants who were plasma donors only for this study are marked in blue. Sequences of variants which were outgrown are marked in yellow. Participant 039-13-0013 was both a plasma donor and the donor from whom the first wave virus was outgrown. Y-axis denotes time of sampling for viral sequencing. Table shows mutations present in Spike for the 501Y.V2 variants and the first wave virus used in the study. See Table S2 for a complete list of mutations in the viral genomes.

We chose plasma from participants from the first infection wave where the infecting virus was successfully sequenced (Table S1) and where RBD binding was detected by ELISA. These viruses were from a variety of B.1 lineages circulating in South Africa and contained the D614G mutation but none of the spike mutations defining 501Y.V2 (Figure 1, see Table S2 for whole genome mutations). Plasma samples were from blood drawn approximately 1 month post-symptom onset (Table S1), shown to be close to the antibody response peak [16, 17].

We outgrew first wave virus (Materials and methods) from a sample obtained from a cohort participant (039-13-0013) in July 2020, and second wave 501Y.V2 virus from two samples obtained in November 2020 through our genomic surveillance program. We used a microneutralization live virus focus forming assay (FFA) [18]. This relies on a methylcellulose overlay to limit cell-free viral spread, resulting in a local infection focus then detected by an anti-SARS-CoV-2 Spike antibody (Materials and methods). Re-sequencing of the first 501Y.V2 variant after outgrowth revealed no changes in the RBD or NTD but a deletion in the furin cleavage site (Table S3) commonly observed after *in vitro* culture in Vero E6 cells [19, 20]. We designated this variant 501Y.V2.HVdF002. HV represents the outgrowth protocol which included initial outgrowth in a human H1299 cell line derivative overexpressing the ACE2 receptor, followed by a cell-to-cell infection of Vero E6 cells (Materials and methods). dF represents the deletion of the furin cleavage site. Deletion of the furin cleavage site may not affect neutralization [19]. However, we proceeded to test an additional 501Y.V2 variant. This variant, which we designated 501Y.V2.HV001, had an additional mutation, L18F, in the NTD prior to outgrowth and showed no changes in spike sequence after outgrowth.

We mixed the virus with serially diluted participant plasma, then added the mixture to Vero E6 cells and counted infection foci after 28 hours (Figure 2A, Materials and methods). There was a clear visual difference in the number of foci as a function of plasma dilution. 501Y.V2.HV001 also showed dramatically larger foci (Figure 2A).

We normalized the number of foci to the number of foci in the absence of plasma on the same plate to obtain the transmission index (Tx, [21]). In this context, it is the number of foci in the presence of plasma inhibition divided by the number of foci in the absence of plasma. This controls for experiment variability between plates and experiments. The data from the FFA approximated a normal distribution (Figure S1) and we therefore used parametric statistics to describe it. We observed neutralization of the first wave virus which varied between plasma samples (Figure 2B). To obtain the IC_{50}, we fitted the data for each participant to a sigmoidal function [22] with IC_{50} as the only free parameter (Materials and methods). Fitted IC_{50} values (Figure 2D) varied between 4×10^{-3} for participant 039-13-0013 to 1×10^{-4} for participants 039-13-0033 and 039-02-0015, consistent with the previously observed heterogeneity in neutralization between individuals [16, 17].

We next determined neutralization of 501Y.V2. A decline in plasma neutralization was clearly observed (Figure 2A). T501Y.V2.HV001 also showed attenuated neutralization likely greater than that of 501Y.V2.HVdF002 (Figure S2), ruling out the *in vitro* generated deletion in the furin cleavage site as being responsible for escape. We combined the data for both 501Y.V2 variants. Fitted IC_{50} values varied between 1×10^{-3} (1:100 dilution) for plasma from participant 039-13-0033 to a complete knock-out of activity for plasma from participant 039-13-0013 (Figure 2D). The 501Y.V2 to first wave IC_{50} ratio ranged from 6 to 200-fold (Figure 2D). Averaging across all participants highlighted the dramatic decrease in sensitivity to neutralization of authentic 501Y.V2 variants (Figure 2E).

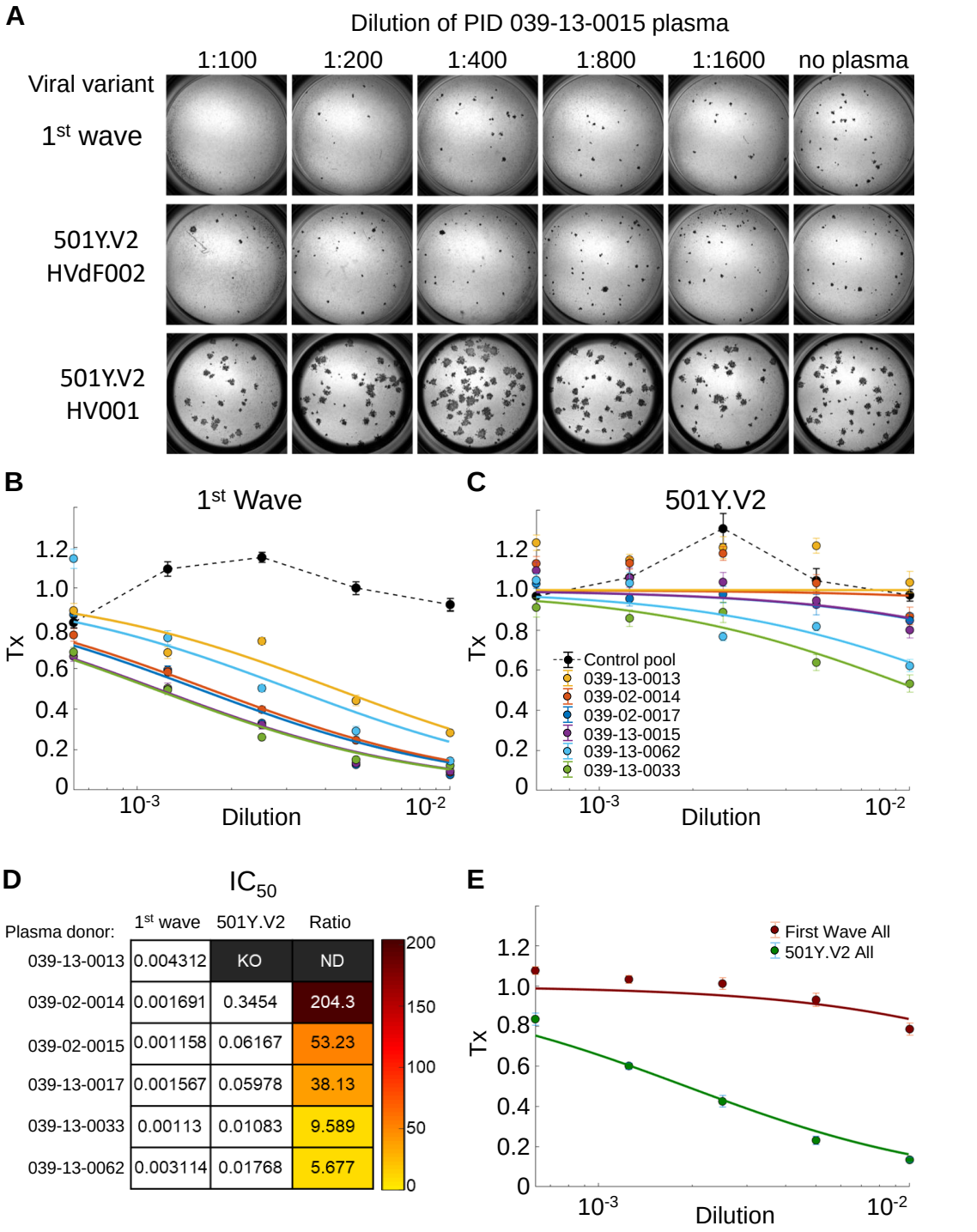

Figure 2: Neutralization of first wave and 501Y.V2 variants by convalescent plasma from first wave infections. (A) A representative focus forming assay using plasma from participant 039-13-0015. Plasma neutralization of (B) first wave virus and (C) the combined results from the two 501Y.V2 variants. Colored circles represent means and standard errors from 8 independent neutralization experiments using plasma from 6 convalescent participants who were infected by first wave variants in the first peak of the pandemic in South Africa. Correspondingly colored lines are fits of the sigmoidal equation with IC_{50} as the fitted parameter. Black points represent a pool of plasma from three uninfected controls. The transmission index (Tx) is the number of foci in the presence of the plasma dilution normalized by the number of foci in the absence of plasma. (D) Plasma IC_{50} values and ratios for first wave and 501Y.V2 variants. Knockout (KO) was scored as $IC_{50} > 1$. ND, not defined. (E) Mean and standard error across all plasma donors.

As we have entered the second year of the SARS-CoV-2 pandemic with high levels of transmission in many parts of the world, variants with mutations at key residues in the spike glycoprotein have emerged. Here we present clear evidence using authentic SARS-CoV-2 that the 501Y.V2 variant first detected in South Africa is associated with reduced neutralization by plasma collected from patients infected in the first wave with SARS-CoV-2 variants without the 501Y.V2 defining RBD and NTD mutations. While our findings are based on plasma samples from six convalescent study participants, the relative consistency of the effect argues that the potential to escape neutralizing antibodies elicited by prior SARS-CoV-2 infection may be widespread.

The reduced neutralization is most likely related to the mutations in the spike RBD and NTD that characterize the 501Y.V2 variant. While the E484K mutation has the clearest association with immune escape, the other mutations in the RBD (K417N, N501Y) are also located within residues targeted by some class 1 and class 2 NAbs [7]. Information about the significance of NTD mutations is also emerging. NAbs targeting this site have been shown to be potent neutralizers of SARS-CoV-2 [5, 6]. The deletion at residues 242-244 is just outside an antigenic supersite loop (residues 245-264) and L18 also falls within the antigenic supersite. Furthermore, mutations at L18 and D80 have been selected during passage with mAbs [5]. Our second variant contains the L18F mutation. This may be associated with the trend to lower neutralization sensitivity relative to the first 501Y.V2 variant (Figure S2). This variant also has strikingly larger foci (Figure 2A).

The reasons for the rapid emergence and fixation of potential immune escape mutations in South Africa remain unclear. The 501Y.V2 variant was first detected in the Eastern Cape Province of South Africa, in Nelson Mandela Bay, an urban municipality with a population of just over one million. While we have no SARS-CoV-2 seroprevalence data from this area, there were 1909 excess natural deaths (approximately 1600 per million population) by the end of the first wave in mid-September (https://www.samrc.ac.za/reports/report-weekly-deaths-south-africa). In the context of a young population (over 80 percent of the population under 50 years), this data would suggest a high attack rate from the first wave. While circumstantial, this provides some support to a hypothesis of high levels of population immunity driving the selection of variants with capacity to evade natural immunity. This area also has high HIV prevalence, and has amongst the lowest proportions of people with HIV who have viral suppression (http://www.hivdata.org.za/). We have not observed evidence of chronic SARS-CoV-2 infection in people living with HIV in our longitudinal cohort [15]. However, most cohort participants had sustained virological suppression with antiretroviral therapy (ART). We did observe altered immune dynamics after SARS-CoV-2 infection in HIV viremic participants relative to those who were virologically suppressed, and we are currently enrolling additional participants to examine SARS-CoV-2 clearance in the HIV viremic subset.

The implications of these results for re-infection and vaccine efficacy are still unclear. Our findings emphasize the need to understand whether the 501Y.V2 variant, and other similar variants, are associated with an increased rate of re-infection. Vaccines such as the Oxford/Astra Zeneca ChAdOx1 [23] and the Pfizer-BioNTech BNT162b2 [24] elicit neutralization titers in a similar range to the convalescent plasma in this study. However, these vaccines may elicit a broader antibody response and protective T cell immunity [25]. Protective T cell immunity also likely occurs following natural infection. Furthermore, it is unclear what degree of neutralization mediates protection, and infection may be particularly sensitive to inhibition at exposure [26].

In conclusion, we present data suggesting that the 501Y.V2 variant first detected in South Africa is able to escape the neutralizing antibody response elicited by natural infection with earlier variants. We expect data in the next weeks from phase 3 vaccine trials being conducted in South Africa. If the variant does have an effect on vaccine efficacy, then there may be a signal in the data from these clinical trials.

Material and methods

Ethical statement

Nasopharyngeal/oropharyngeal swab samples and plasma samples were obtained from six hospitalized adults with PCR-confirmed SARS-CoV-2 infection enrolled in a prospective cohort study approved by the Biomedical Research Ethics Committee (BREC) at the University of KwaZulu-Natal (reference BREC/00001275/2020). The 501Y.V2 variants were obtained from residual nasopharyngeal/oropharyngeal samples used for routine SARS-CoV-2 diagnostic testing by the National Health Laboratory Service, through our SARS-CoV-2 genomic surveillance program (BREC approval reference BREC/00001510/2020).

Whole genome sequencing, genome assembly and phylogenetic analysis

cDNA synthesis was performed on the extracted RNA using random primers followed by gene specific multiplex PCR using the ARTIC V3 protocol. Briefly, extracted RNA was converted to cDNA using the Superscript IV First Strand synthesis system (Life Technologies, Carlsbad, CA) and random hexamer primers. SARS-CoV-2 whole genome amplification was performed by multiplex PCR using primers designed on Primal Scheme (http://primal.zibraproject.org/) to generate 400bp amplicons with an overlap of 70bp that covers the 30Kb SARS-CoV-2 genome. PCR products were cleaned up using AmpureXP purification beads (Beckman Coulter, High Wycombe, UK) and quantified using the Qubit dsDNA High Sensitivity assay on the Qubit 4.0 instrument (Life Technologies Carlsbad, CA). We then used the Illumina® Nextera Flex DNA Library Prep kit according to the manufacturer's protocol to prepare indexed paired end libraries of genomic DNA. Sequencing libraries were normalized to 4nM, pooled and denatured with 0.2N sodium acetate. 12pM sample library was spiked with 1% PhiX (PhiX Control v3 adapter-ligated library used as a control). We sequenced libraries on a 500-cycle v2 MiSeq Reagent Kit on the Illumina MiSeq instrument (Illumina, San Diego, CA). We have previously published full details of the amplification and sequencing protocol [27].

We assembled paired-end fastq reads using Genome Detective 1.126 (https://www.genomedetective.com) and the Coronavirus Typing Tool [28]. We polished the initial assembly obtained from Genome Detective by aligning mapped reads to the references and filtering out low-quality mutations using bcftools 1.7-2 mpileup method. Mutations were confirmed visually with bam files using Geneious software (Biomatters Ltd, Auckland, New Zealand). All of the sequences were deposited in GISAID (https://www.gisaid.org/). We retrieved all South African SARS-CoV-2 genotypes from the GISAID database as of 11 January 2021 (N=2704). We initially analyzed South African genotypes against the global reference dataset (N=2592) using a custom pipeline based on a local version of NextStrain. The pipeline contains several python scripts that manage the analysis workflow. It performs alignment of genotypes in MAFFT [29], phylogenetic tree inference in IQ-Tree20, tree dating and ancestral state construction and annotation (https://github.com/nextstrain/ncov).

Cells

Vero E6 cells (ATCC CRL-1586, obtained from Cellonex) were propagated in complete DMEM with 10% fetal bovine serum (Hylone) containing 1% each of HEPES, sodium pyruvate, L-glutamine, and non-essential amino acids (Sigma-Aldrich). Cells were passaged every 3-4 days. H1299 cells were propagated in complete RPMI with 10% fetal bovine serum containing 1% each of HEPES, sodium pyruvate, L-glutamine, and non-essential amino acids and and passaged every second day.

H1299-E3 cell line for first passage SARS-CoV-2 outgrowth

The H1299-H2AZ clone with nuclear labelled YFP [30] was constructed to overexpress ACE2 as follows: VSVG-pseudotyped lentivirus containing the human ACE2 was generated by co-transfecting 293T cells with the pHAGE2-EF1alnt-ACE2-WT plasmid along with the lentiviral helper plasmids HDM-VSVG,

HDM-Hgpm2, HDM-tat1b and pRC-CMV-Rev1b using TransIT-LT1 (Mirus) transfection reagent. Supernatant containing the lentivirus was harvested two days after infection, filtered through a 0.45μm filter (Corning) and used to spinfect H1299-H2AZ at 1000 rcf for 2 hours at room temperature in the presence of 5 μg/mL polybrene (Sigma-Aldrich). ACE-2 transduced H1299-H2AZ cells were then subcloned at the single cell density in 96-well plates (Eppendorf) in conditioned media derived from confluent cells. After 3 weeks, wells were trypsinized (Sigma-Aldrich) and plated in two replicate plates, where the first plate was used to determine infectivity and the second was stock. The first plate was screened for the fraction of mCherry positive cells per cell clone upon infection with SARS-CoV-2 mCherry expressing Spike pseudotyped lentiviral vector 1610-pHAGE2/EF1a Int-mCherry3-W produced by transfecting as above. Screening was performed using a Metamorph-controlled (Molecular Devices, Sunnyvale, CA) Nikon TiE motorized microscope (Nikon Corporation, Tokyo, Japan) with a 20x, 0.75 NA phase objective, 561 laser line, and 607 nm emission filter (Semrock, Rochester, NY). Images were captured using an 888 EMCCD camera (Andor). Temperature (37°C), humidity and CO2 (5%) were controlled using an environmental chamber (OKO Labs, Naples, Italy). The clone with the highest fraction of mCherry expression was expanded from the stock plate and denoted H1299-E3. This clone was used in the outgrowth.

Viral Outgrowth

All live virus work was performed in Biosafety level 3 containment using AHRI Institutional Biosafety Committee approved protocols for SARS-CoV-2. For first wave virus, a T25 flask (Corning) was seeded with Vero E6 cells at 2×10^5 cells/ml and incubated for 18-20 hours. After 1 DPBS wash, the sub-confluent cell monolayer was inoculated with 500μL universal transport medium (UTM) diluted 1:1 with growth medium and filtered through a 0.45μM filter. Cells were incubated for 1 hour. Flask was then filled with 7mL of complete growth medium and checked daily for cytopathic effect (CPE). Four days post infection, supernatants of the infected culture were collected, centrifuged at 300 rcf for 3 minutes to remove cell debris, and filtered using a 0.45μM filter. Viral supernatant was aliquoted and stored at -80°C. For 501Y.V2 variants, we used H1299-ACE2-E3 cells for initial isolation followed by passage into Vero E6 cells. H1299-ACE2-E3 cells were seeded at 1.5×10^5 cells/ml and incubated for 18-20 hours. After 1 DPBS wash, the sub-confluent cell monolayer was inoculated with 500μL universal transport medium (UTM) diluted 1:1 with growth medium and filtered through a 0.45μM filter. Cells were incubated for 1 hour. Wells were then filled with 3mL of complete growth medium. 8 days post-infection, cells were trypsinized, centrifuged at 300 rcf for 3 minutes and resuspended in 4mL growth medium. 1mL was added to Vero E6 cells that had been seeded at t 2×10^5 cells/ml 18-20 hours earlier in a T25 flask (approximately 1:8 donor-to-target cell dilution ratio) for cell-to-cell infection. Coculture of H1299-ACE2-E3 and Vero E6 cells was incubated for 1 hour and flask was then filled with 7mL of complete growth medium and incubated for 6 days. Viral supernatant was aliquoted and stored at -80°C or further passaged in Vero E6 cells as above.

Microneutralization using focus forming assay

Vero E6 cells were plated in an 96 well plate (Eppendorf) at 30,000 cells per well 1 day pre-infection. Plasma was separated from EDTA-anticoagulated blood by centrifugation at 500 rcf for 10 minutes and stored at -80°C. Aliquots of plasma samples were heat-inactivated at 56°C for 30 minutes, and clarified by centrifugation at 10,000 rcf for 5 minutes, where the clear middle layer was used for experiments. Inactivated plasma was stored in single use aliquots to prevent freeze-thaw cycles. For experiments, plasma was serially diluted two-fold from 1:100 to 1:1600. Virus stocks were used at approximately 50 focus-forming units (FFU) per microwell and added to diluted plasma; antibody-virus mixtures were incubated for 1 hour at 37°C, 5% CO2 . Cells were infected with 100μL of the virus-antibody mixtures, to allow adsorption of virus. Subsequently, 100μL of a 1x RPMI 1640 (Sigma-Aldrich R6504), 1.5% carboxymethylcellulose (Sigma-Aldrich C4888) overlay was added to the wells without removing the inoculum. Cells were fixed at 28 hours post-infection using 4% paraformaldehyde (Sigma-Aldrich) for 20 minutes. For staining of foci, a rabbit anti-Spike monoclonal antibody (mAb BS-R2B12, GenScript

A02058) was used at 0.5μg/mL as the primary detection antibody. Antibody was resuspended in a permiabilization buffer containing 0.1% saponin (Sigma-Aldrich), 0.1% BSA (Sigma-Aldrich), and 0.05% tween (Sigma-Aldrich) in PBS. Plates were incubated with primary antibody overnight at 4°C, then washed with wash buffer containing 0.05% tween in PBS. Secondary goat anti-rabbit horseradish peroxidase (Abcam ab205718) was added at 1 μg/mL and incubated for 2 hours at room temperature with shaking. The TrueBlue peroxidase substrate (SeraCare 5510-0030) was then added at 50μL per well and incubated for 20 minutes at room temperature. Plates were then dried for 2 hours and imaged using a Metamorph-controlled Nikon TiE motorized microscope with a 2x objective. Automated image analysis was performed using a Matlab2019b (Mathworks) custom script, where focus detection was automated and did not involve user curation. Image segmentation steps were stretching the image from minimum to maximum intensity, local Laplacian filtering, image complementation, thresholding and binarization. For the second 501Y.V2 variant, a dilation/erosion step was introduced to prevent the large foci from fragmenting into smaller objects.

Statistics and fitting

All statistics and fitting were performed using Matlab2019b. Neutralization data was fit to

$$Tx = 1/1 + (D/IC_{50}).$$

Here Tx is the number of foci normalized to the number of foci in the absence of plasma on the same plate at dilution D. Fit to a normal distribution using Matlab2019b function normplot, which compared the distribution of the Tx data to the normal distribution (see https://www.mathworks.com/help/stats/normplot.html).

Acknowledgements

This work was supported by the Bill and Melinda Gates Investment INV-018944 (AS) and by the South African Medical Research Council and the Department of Science and Innovation (TdO).

§ Network for Genomic Surveillance in South Africa (NGS-SA)

Shareef Abrahams[1], Luiz Carlos Junior Alcantara[2], Arghavan Alisoltani-Dehkordi[3,4], Mushal Allam[5], Jinal N Bhiman[5,6], Mary-Ann Davies[7,8], Deelan Doolabh[9], Susan Engelbrecht[10], Vagner Fonseca[11], Marta Giovanetti[2], Allison J Glass[6,12], Adam Godzik[4], Dominique Goedhals[13], Diana Hardie[14], Marvin Hsiao[14], Arash Iranzadeh[4], Arshad Ismail[5], Stephen Korsman[14], Sergei L Kosakovsky Pond[15], Oluwakemi Laguda-Akingba[1,16], Jose Lourenco[17], Gert Marais[14], Darren Martin[9,18], Caroline Maslo[19], Koleka Mlisana[20,21], Thabo Mohale[5], Nokukhanya Msomi[22], Innocent Mudau[9], Francesco Petruccione[23,24], Wolfgang Preiser[10], Emmanuel James San[11], Bryan Trevor Sewell[25], Lynn Tyers[9], Gert Van Zyl[10], Anne von Gottberg[5,6], Sibongile Walaza[5,26], Steven Weaver[15], Constantinos Kurt Wibmer[5], Carolyn Williamson[9,14,21], Denis York[27].

[1]National Health Laboratory Service, Port Elizabeth, South Africa. [2]Laboratorio de Flavivirus, Fundacao Oswaldo Cruz, Rio de Janeiro, Brazil. [3]Division of Medical Virology, Department of Pathology, University of Cape Town, Cape Town, South Africa. [4]Division of Biomedical Sciences, University of California Riverside School of Medicine, Riverside, California, USA. [5]National Institute for Communicable Diseases of the National Health Laboratory Service, Johannesburg, South Africa. [6]School of Pathology, Faculty of Health Sciences, University of the Witwatersrand, Johannesburg, South Africa. [7]Centre for Infectious Disease Epidemiology and Research, University of Cape Town, Cape Town, South Africa. [8]Western Cape Government: Health, Cape Town, South Africa. [9]Division of Medical Virology, Institute of Infectious Disease and Molecular Medicine, University of Cape Town, Cape Town, South Africa. [10]Division of Medical Virology at NHLS Tygerberg Hospital and Faculty of Medicine and Health Sciences, Stellenbosch University, Cape Town, South Africa. [11]KwaZulu-Natal Research Innovation and

Sequencing Platform (KRISP), Department of Laboratory Medicine and Medical Sciences, University of KwaZulu-Natal, Durban, South Africa. [12]Department of Molecular Pathology, Lancet Laboratories, Johannesburg, South Africa. [13]Division of Virology at NHLS Universitas Academic Laboratories, University of The Free State, Bloemfontein, South Africa. [14]Division of Medical Virology at NHLS Groote Schuur Hospital, University of Cape Town, Cape Town, South Africa. [15]Institute for Genomics and Evolutionary Medicine, Temple University, Philadelphia, Pennsylvania, USA. [16]Department of Laboratory Medicine and Pathology, Faculty of Health Sciences, Walter Sisulu University, Mthatha, South Africa. [17]Department of Zoology, University of Oxford, Oxford, United Kingdom. [18]Computational Biology Division, Department of Integrative Biomedical Sciences, University of Cape Town, Cape Town, South Africa. [19]Department of Quality Leadership, Netcare Hospitals, Johannesburg, South Africa. [20]National Health Laboratory Service, Johannesburg, South Africa. [21]Centre for the AIDS Programme of Research in South Africa (CAPRISA), Durban, South Africa. [22]Discipline of Virology, University of KwaZulu-Natal, School of Laboratory Medicine and Medical Sciences and National Health Laboratory Service, Durban, South Africa. [23]Centre for Quantum Technology, University of KwaZulu-Natal, Durban, South Africa [24]National Institute for Theoretical Physics (NITheP), KwaZulu-Natal, South Africa. [25]Structural Biology Research Unit, Department of Integrative Biomedical Sciences, University of Cape Town, Rondebosch, South Africa. [26]School of Public Health, Faculty of Health Sciences, University of the Witwatersrand, Johannesburg, South Africa. [27]Molecular Diagnostics Services, Durban, South Africa.

§ § COMMIT-KZN Team

Moherndran Archary[1], Kaylesh J. Dullabh[2], Philip Goulder[3,4], Guy Harling[3,5], Rohen Harrichandparsad[6], Kobus Herbst[3,7], Prakash Jeena[1], Thandeka Khoza[3], Nigel Klein[3,8], Henrik Kløverpris[3,9,10], Alasdair Leslie[3,9], Rajhmun Madansein[2], Mohlopheni Marakalala[3,9], Matilda Mazibuko[3], Mosa Moshabela[11], Ntombifuthi Mthabela[3], Kogie Naidoo[12], Zaza Ndhlovu[3,13], Thumbi Ndung'u[3,9,14,15], Kennedy Nyamande[16], Nesri Padayatchi[12], Vinod Patel[17], Theresa Smit[3], Adrie Steyn[3,18], Emily Wong[3,18].

[1]Department of Paediatrics and Child Health, University of KwaZulu-Natal, Durban, South Africa. [2]Department of Cardiothoracic Surgery, University of KwaZulu-Natal, Durban, South Africa. [3]Africa Health Research Institute, Durban, South Africa. [4]Department of Paediatrics, Oxford, UK. [5]Institute for Global Health, University College London, UK. [6]Department of Neurosurgery, University of KwaZulu-Natal, Durban, South Africa. [7]South African Population Research Infrastructure Network, Durban, South Africa. [8]Institute of Child Health, University College London, UK. [9]Division of Infection and Immunity, University College London, London, UK. [10]Department of Immunology and Microbiology, University of Copenhagen, Copenhagen, Denmark. [11]College of Health Sciences, University of KwaZulu-Natal, Durban, South Africa. [12]Centre for the AIDS Programme of Research in South Africa, Durban, South Africa. [13]Ragon Institute of MGH, MIT and Harvard, Boston, USA. [14]HIV Pathogenesis Programme, The Doris Duke Medical Research Institute, University of KwaZulu-Natal, Durban, South Africa. [15]Max Planck Institute for Infection Biology, Berlin, Germany. [16]Department of Pulmonology and Critical Care, University of KwaZulu-Natal, Durban, South Africa. [17]Department of Neurology, University of KwaZulu-Natal, Durban, South Africa. [18]Division of Infectious Diseases, University of Alabama at Birmingham.

References

[1] Houriiyah Tegally, Eduan Wilkinson, Marta Giovanetti, Arash Iranzadeh, Vagner Fonseca, Jennifer Giandhari, Deelan Doolabh, Sureshnee Pillay, Emmanuel James San, Nokukhanya Msomi, Koleka Mlisana, Anne von Gottberg, Sibongile Walaza, Mushal Allam, Arshad Ismail, Thabo Mohale, Allison J Glass, Susan Engelbrecht, Gert Van Zyl, Wolfgang Preiser, Francesco Petruccione, Alex Sigal, Diana Hardie, Gert Marais, Marvin Hsiao, Stephen Korsman, Mary-

Ann Davies, Lynn Tyers, Innocent Mudau, Denis York, Caroline Maslo, Dominique Goedhals, Shareef Abrahams, Oluwakemi Laguda-Akingba, Arghavan Alisoltani-Dehkordi, Adam Godzik, Constantinos Kurt Wibmer, Bryan Trevor Sewell, José Lourenço, Luiz Carlos Junior Alcantara, Sergei L Kosakovsky Pond, Steven Weaver, Darren Martin, Richard J Lessells, Jinal N Bhiman, Carolyn Williamson, and Tulio de Oliveira. Emergence and rapid spread of a new severe acute respiratory syndrome-related coronavirus 2 (sars-cov-2) lineage with multiple spike mutations in south africa. *medRxiv*, page 2020.12.21.20248640, 2020. doi: 10.1101/2020.12.21.20248640. URL `https://www.medrxiv.org/content/medrxiv/early/2020/12/22/2020.12.21.20248640.full.pdf`.

[2] Erik Volz, Swapnil Mishra, Meera Chand, Jeffrey C. Barrett, Robert Johnson, Lily Geidelberg, Wes R Hinsley, Daniel J Laydon, Gavin Dabrera, Áine O'Toole, Roberto Amato, Manon Ragonnet-Cronin, Ian Harrison, Ben Jackson, Cristina V. Ariani, Olivia Boyd, Nick Loman, John T McCrone, Sónia Gonçalves, David Jorgensen, Richard Myers, Verity Hill, David K. Jackson, Katy Gaythorpe, Natalie Groves, John Sillitoe, Dominic P. Kwiatkowski, Seth Flaxman, Oliver Ratmann, Samir Bhatt, Susan Hopkins, Axel Gandy, Andrew Rambaut, and Neil M Ferguson. Transmission of sars-cov-2 lineage b.1.1.7 in england: Insights from linking epidemiological and genetic data. *medRxiv*, page 2020.12.30.20249034, 2021. doi: 10.1101/2020.12.30.20249034. URL `https://www.medrxiv.org/content/medrxiv/early/2021/01/04/2020.12.30.20249034.full.pdf`.

[3] Carolina M Voloch, Ronaldo da Silva F, Luiz G P de Almeida, Cynthia C Cardoso, Otavio J. Brustolini, Alexandra L Gerber, Ana Paula de C Guimarães, Diana Mariani, Raissa Mirella da Costa, Orlando C. Ferreira, Adriana Cony Cavalcanti, Thiago Silva Frauches, Claudia Maria Braga de Mello, Rafael Mello Galliez, Débora Souza Faffe, Terezinha M P P Castiñeiras, Amilcar Tanuri, and Ana Tereza R de Vasconcelos. Genomic characterization of a novel sars-cov-2 lineage from rio de janeiro, brazil. *medRxiv*, page 2020.12.23.20248598, 2020. doi: 10.1101/2020.12.23.20248598. URL `https://www.medrxiv.org/content/medrxiv/early/2020/12/26/2020.12.23.20248598.full.pdf`.

[4] L. Piccoli, Y. J. Park, M. A. Tortorici, N. Czudnochowski, A. C. Walls, M. Beltramello, C. Silacci-Fregni, D. Pinto, L. E. Rosen, J. E. Bowen, O. J. Acton, S. Jaconi, B. Guarino, A. Minola, F. Zatta, N. Sprugasci, J. Bassi, A. Peter, A. De Marco, J. C. Nix, F. Mele, S. Jovic, B. F. Rodriguez, S. V. Gupta, F. Jin, G. Piumatti, G. Lo Presti, A. F. Pellanda, M. Biggiogero, M. Tarkowski, M. S. Pizzuto, E. Cameroni, C. Havenar-Daughton, M. Smithey, D. Hong, V. Lepori, E. Albanese, A. Ceschi, E. Bernasconi, L. Elzi, P. Ferrari, C. Garzoni, A. Riva, G. Snell, F. Sallusto, K. Fink, H. W. Virgin, A. Lanzavecchia, D. Corti, and D. Veesler. Mapping neutralizing and immunodominant sites on the sars-cov-2 spike receptor-binding domain by structure-guided high-resolution serology. *Cell*, 183(4):1024–1042 e21, 2020. ISSN 1097-4172 (Electronic) 0092-8674 (Linking). doi: 10.1016/j.cell.2020.09.037. URL `https://www.ncbi.nlm.nih.gov/pubmed/32991844`.

[5] Matthew McCallum, Anna De Marco, Florian Lempp, M. Alejandra Tortorici, Dora Pinto, Alexandra C. Walls, Martina Beltramello, Alex Chen, Zhuoming Liu, Fabrizia Zatta, Samantha Zepeda, Julia di Iulio, John E. Bowen, Martin Montiel-Ruiz, Jiayi Zhou, Laura E. Rosen, Siro Bianchi, Barbara Guarino, Chiara Silacci Fregni, Rana Abdelnabi, Shi-Yan Caroline Foo, Paul W. Rothlauf, Louis-Marie Bloyet, Fabio Benigni, Elisabetta Cameroni, Johan Neyts, Agostino Riva, Gyorgy Snell, Amalio Telenti, Sean P.J. Whelan, Herbert W. Virgin, Davide Corti, Matteo Samuele Pizzuto, and David Veesler. N-terminal domain antigenic mapping reveals a site of vulnerability for sars-cov-2. *bioRxiv*, page 2021.01.14.426475, 2021. doi: 10.1101/2021.01.14.426475. URL `https://www.biorxiv.org/content/biorxiv/early/2021/01/14/2021.01.14.426475.full.pdf`.

[6] Gabriele Cerutti, Yicheng Guo, Tongqing Zhou, Jason Gorman, Myungjin Lee, Micah Rapp, Eswar R. Reddem, Jian Yu, Fabiana Bahna, Jude Bimela, Yaoxing Huang, Phinikoula S. Katsamba, Lihong Liu, Manoj S. Nair, Reda Rawi, Adam S. Olia, Pengfei Wang, Gwo-Yu Chuang, David D. Ho, Zizhang Sheng, Peter D. Kwong, and Lawrence Shapiro. Potent sars-cov-2 neutralizing antibodies directed against spike n-terminal domain target a single supersite. *bioRxiv*, page 2021.01.10.426120, 2021. doi: 10.1101/2021.01.10.426120. URL `https://www.biorxiv.org/content/biorxiv/early/2021/01/11/2021.01.10.426120.full.pdf`.

[7] C. O. Barnes, C. A. Jette, M. E. Abernathy, K. A. Dam, S. R. Esswein, H. B. Gristick, A. G. Malyutin, N. G. Sharaf, K. E. Huey-Tubman, Y. E. Lee, D. F. Robbiani, M. C. Nussenzweig, Jr. West, A. P., and P. J. Bjorkman. Sars-cov-2 neutralizing antibody structures inform therapeutic strategies. *Nature*, 588(7839):682–687, 2020. ISSN 1476-4687 (Electronic) 0028-0836 (Linking). doi: 10.1038/s41586-020-2852-1. URL `https://www.ncbi.nlm.nih.gov/pubmed/33045718`.

[8] Alina Baum, Benjamin O Fulton, Elzbieta Wloga, Richard Copin, Kristen E Pascal, Vincenzo Russo, Stephanie Giordano, Kathryn Lanza, Nicole Negron, and Min Ni. Antibody cocktail to sars-cov-2 spike protein prevents rapid mutational escape seen with individual antibodies. *Science*, 369(6506):1014–1018, 2020. ISSN 0036-8075.

[9] A. J. Greaney, T. N. Starr, P. Gilchuk, S. J. Zost, E. Binshtein, A. N. Loes, S. K. Hilton, J. Huddleston, R. Eguia, K. H. D. Crawford, A. S. Dingens, R. S. Nargi, R. E. Sutton, N. Suryadevara, P. W. Rothlauf, Z. Liu, S. P. J. Whelan, R. H. Carnahan, Jr. Crowe, J. E., and J. D. Bloom. Complete mapping of mutations to the sars-cov-2 spike receptor-binding domain that escape antibody recognition. *Cell Host Microbe*, 2020. ISSN 1934-6069 (Electronic) 1931-3128 (Linking). doi: 10.1016/j.chom.2020.11.007. URL `https://www.ncbi.nlm.nih.gov/pubmed/33259788`.

[10] Z. Liu, H. Zheng, H. Lin, M. Li, R. Yuan, J. Peng, Q. Xiong, J. Sun, B. Li, J. Wu, L. Yi, X. Peng, H. Zhang, W. Zhang, R. J. G. Hulswit, N. Loman, A. Rambaut, C. Ke, T. A. Bowden, O. G. Pybus, and J. Lu. Identification of common deletions in the spike protein of severe acute respiratory syndrome coronavirus 2. *J Virol*, 94(17), 2020. ISSN 1098-5514 (Electronic) 0022-538X (Linking). doi: 10.1128/JVI.00790-20. URL `https://www.ncbi.nlm.nih.gov/pubmed/32571797`.

[11] Y. Weisblum, F. Schmidt, F. Zhang, J. DaSilva, D. Poston, J. C. Lorenzi, F. Muecksch, M. Rutkowska, H. H. Hoffmann, E. Michailidis, C. Gaebler, M. Agudelo, A. Cho, Z. Wang, A. Gazumyan, M. Cipolla, L. Luchsinger, C. D. Hillyer, M. Caskey, D. F. Robbiani, C. M. Rice, M. C. Nussenzweig, T. Hatziioannou, and P. D. Bieniasz. Escape from neutralizing antibodies by sars-cov-2 spike protein variants. *Elife*, 9, 2020. ISSN 2050-084X (Electronic) 2050-084X (Linking). doi: 10.7554/eLife.61312. URL `https://www.ncbi.nlm.nih.gov/pubmed/33112236`.

[12] E. Andreano, G. Piccini, D. Licastro, L. Casalino, N. V. Johnson, I. Paciello, S. D. Monego, E. Pantano, N. Manganaro, A. Manenti, R. Manna, E. Casa, I. Hyseni, L. Benincasa, E. Montomoli, R. E. Amaro, J. S. McLellan, and R. Rappuoli. Sars-cov-2 escape in vitro from a highly neutralizing covid-19 convalescent plasma. *bioRxiv*, 2020. doi: 10.1101/2020.12.28.424451. URL `https://www.ncbi.nlm.nih.gov/pubmed/33398278`.

[13] Zhuoming Liu, Laura A. VanBlargan, Louis-Marie Bloyet, Paul W. Rothlauf, Rita E. Chen, Spencer Stumpf, Haiyan Zhao, John M. Errico, Elitza S. Theel, Mariel J. Liebeskind, Brynn Alford, William J. Buchser, Ali H. Ellebedy, Daved H. Fremont, Michael S. Diamond, and Sean P. J. Whelan. Landscape analysis of escape variants identifies sars-cov-2 spike mutations that attenuate monoclonal and serum antibody neutralization. *bioRxiv*, page 2020.11.06.372037, 2021. doi: 10.1101/2020.11.06.372037. URL `https://www.biorxiv.org/content/biorxiv/early/2021/01/11/2020.11.06.372037.full.pdf`.

[14] Allison J Greaney, Andrea N Loes, Katharine HD Crawford, Tyler N Starr, Keara D Malone, Helen Y Chu, and Jesse D Bloom. Comprehensive mapping of mutations to the sars-cov-2 receptor-binding domain that affect recognition by polyclonal human serum antibodies. *bioRxiv*, page 2020.12. 31.425021, 2021.

[15] Farina Karim, Inbal Gazy, Sandile Cele, Yenzekile Zungu, Robert Krause, Mallory Bernstein, Yashica Ganga, Hylton Rodel, Ntombifuthi Mthabela, Matilda Mazibuko, Khadija Khan, Daniel Muema, Dirhona Ramjit, Gila Lustig, Thumbi Ndung'u, Willem Hanekom, Bernadett I. Gosnell, Emily Wong, Tulio de Oliveira, Mahomed-Yunus S. Moosa, Alasdair Leslie, Henrik Kløverpris, and Alex Sigal. Hiv infection alters sars-cov-2 responsive immune parameters but not clinical outcomes in covid-19 disease.

medRxiv, page 2020.11.23.20236828, 2020. doi: 10.1101/2020.11.23.20236828. URL https://www.medrxiv.org/content/medrxiv/early/2020/11/24/2020.11.23.20236828.full.pdf.

[16] D. F. Robbiani, C. Gaebler, F. Muecksch, J. C. C. Lorenzi, Z. Wang, A. Cho, M. Agudelo, C. O. Barnes, A. Gazumyan, S. Finkin, T. Hagglof, T. Y. Oliveira, C. Viant, A. Hurley, H. H. Hoffmann, K. G. Millard, R. G. Kost, M. Cipolla, K. Gordon, F. Bianchini, S. T. Chen, V. Ramos, R. Patel, J. Dizon, I. Shimeliovich, P. Mendoza, H. Hartweger, L. Nogueira, M. Pack, J. Horowitz, F. Schmidt, Y. Weisblum, E. Michailidis, A. W. Ashbrook, E. Waltari, J. E. Pak, K. E. Huey-Tubman, N. Koranda, P. R. Hoffman, Jr. West, A. P., C. M. Rice, T. Hatziioannou, P. J. Bjorkman, P. D. Bieniasz, M. Caskey, and M. C. Nussenzweig. Convergent antibody responses to sars-cov-2 in convalescent individuals. *Nature*, 584(7821):437–442, 2020. ISSN 1476-4687 (Electronic) 0028-0836 (Linking). doi: 10.1038/s41586-020-2456-9. URL https://www.ncbi.nlm.nih.gov/pubmed/32555388.

[17] C. Gaebler, Z. Wang, J. C. C. Lorenzi, F. Muecksch, S. Finkin, M. Tokuyama, A. Cho, M. Jankovic, D. Schaefer-Babajew, T. Y. Oliveira, M. Cipolla, C. Viant, C. O. Barnes, Y. Bram, G. Breton, T. Hagglof, P. Mendoza, A. Hurley, M. Turroja, K. Gordon, K. G. Millard, V. Ramos, F. Schmidt, Y. Weisblum, D. Jha, M. Tankelevich, G. Martinez-Delgado, J. Yee, R. Patel, J. Dizon, C. Unson-O'Brien, I. Shimeliovich, D. F. Robbiani, Z. Zhao, A. Gazumyan, R. E. Schwartz, T. Hatziioannou, P. J. Bjorkman, S. Mehandru, P. D. Bieniasz, M. Caskey, and M. C. Nussenzweig. Evolution of antibody immunity to sars-cov-2, 2021. ISSN 1476-4687 (Electronic) 0028-0836 (Linking). URL https://www.ncbi.nlm.nih.gov/pubmed/33461210.

[18] James Brett Case, Adam L Bailey, Arthur S Kim, Rita E Chen, and Michael S Diamond. Growth, detection, quantification, and inactivation of sars-cov-2. *Virology*, 2020.

[19] W. B. Klimstra, N. L. Tilston-Lunel, S. Nambulli, J. Boslett, C. M. McMillen, T. Gilliland, M. D. Dunn, C. Sun, S. E. Wheeler, A. Wells, A. L. Hartman, A. K. McElroy, D. S. Reed, L. J. Rennick, and W. P. Duprex. Sars-cov-2 growth, furin-cleavage-site adaptation and neutralization using serum from acutely infected hospitalized covid-19 patients. *J Gen Virol*, 101(11):1156–1169, 2020. ISSN 1465-2099 (Electronic) 0022-1317 (Linking). doi: 10.1099/jgv.0.001481. URL https://www.ncbi.nlm.nih.gov/pubmed/32821033.

[20] A. C. Walls, Y. J. Park, M. A. Tortorici, A. Wall, A. T. McGuire, and D. Veesler. Structure, function, and antigenicity of the sars-cov-2 spike glycoprotein. *Cell*, 181(2):281–292 e6, 2020. ISSN 1097-4172 (Electronic) 0092-8674 (Linking). doi: 10.1016/j.cell.2020.02.058. URL https://www.ncbi.nlm.nih.gov/pubmed/32155444.

[21] A. Sigal, J. T. Kim, A. B. Balazs, E. Dekel, A. Mayo, R. Milo, and D. Baltimore. Cell-to-cell spread of hiv permits ongoing replication despite antiretroviral therapy. *Nature*, 477(7362):95–8, 2011. ISSN 1476-4687 (Electronic) 0028-0836 (Linking). doi: 10.1038/nature10347. URL https://www.ncbi.nlm.nih.gov/pubmed/21849975.

[22] L. Shen, S. Peterson, A. R. Sedaghat, M. A. McMahon, M. Callender, H. Zhang, Y. Zhou, E. Pitt, K. S. Anderson, E. P. Acosta, and R. F. Siliciano. Dose-response curve slope sets class-specific limits on inhibitory potential of anti-hiv drugs. *Nat Med*, 14(7):762–6, 2008. ISSN 1546-170X (Electronic) 1078-8956 (Linking). doi: 10.1038/nm1777. URL https://www.ncbi.nlm.nih.gov/pubmed/18552857.

[23] M. N. Ramasamy, A. M. Minassian, K. J. Ewer, A. L. Flaxman, P. M. Folegatti, D. R. Owens, M. Voysey, P. K. Aley, B. Angus, G. Babbage, S. Belij-Rammerstorfer, L. Berry, S. Bibi, M. Bittaye, K. Cathie, H. Chappell, S. Charlton, P. Cicconi, E. A. Clutterbuck, R. Colin-Jones, C. Dold, K. R. W. Emary, S. Fedosyuk, M. Fuskova, D. Gbesemete, C. Green, B. Hallis, M. M. Hou, D. Jenkin, C. C. D. Joe, E. J. Kelly, S. Kerridge, A. M. Lawrie, A. Lelliott, M. N. Lwin, R. Makinson, N. G. Marchevsky, Y. Mujadidi, A. P. S. Munro, M. Pacurar, E. Plested, J. Rand, T. Rawlinson, S. Rhead, H. Robinson, A. J. Ritchie, A. L. Ross-Russell, S. Saich, N. Singh,

C. C. Smith, M. D. Snape, R. Song, R. Tarrant, Y. Themistocleous, K. M. Thomas, T. L. Villafana, S. C. Warren, M. E. E. Watson, A. D. Douglas, A. V. S. Hill, T. Lambe, S. C. Gilbert, S. N. Faust, A. J. Pollard, and Covid Vaccine Trial Group Oxford. Safety and immunogenicity of chadox1 ncov-19 vaccine administered in a prime-boost regimen in young and old adults (cov002): a single-blind, randomised, controlled, phase 2/3 trial. *Lancet*, 396(10267):1979–1993, 2021. ISSN 1474-547X (Electronic) 0140-6736 (Linking). doi: 10.1016/S0140-6736(20)32466-1. URL `https://www.ncbi.nlm.nih.gov/pubmed/33220855`.

[24] E. E. Walsh, Jr. Frenck, R. W., A. R. Falsey, N. Kitchin, J. Absalon, A. Gurtman, S. Lockhart, K. Neuzil, M. J. Mulligan, R. Bailey, K. A. Swanson, P. Li, K. Koury, W. Kalina, D. Cooper, C. Fontes-Garfias, P. Y. Shi, O. Tureci, K. R. Tompkins, K. E. Lyke, V. Raabe, P. R. Dormitzer, K. U. Jansen, U. Sahin, and W. C. Gruber. Safety and immunogenicity of two rna-based covid-19 vaccine candidates. *N Engl J Med*, 383(25):2439–2450, 2020. ISSN 1533-4406 (Electronic) 0028-4793 (Linking). doi: 10.1056/NEJMoa2027906. URL `https://www.ncbi.nlm.nih.gov/pubmed/33053279`.

[25] Alba Grifoni, Daniela Weiskopf, Sydney I Ramirez, Jose Mateus, Jennifer M Dan, Carolyn Rydyznski Moderbacher, Stephen A Rawlings, Aaron Sutherland, Lakshmanane Premkumar, and Ramesh S Jadi. Targets of t cell responses to sars-cov-2 coronavirus in humans with covid-19 disease and unexposed individuals. *Cell*, 2020. ISSN 0092-8674.

[26] A. Moyano, G. Lustig, H. E. Rodel, T. Antal, and A. Sigal. Interference with hiv infection of the first cell is essential for viral clearance at sub-optimal levels of drug inhibition. *PLoS Comput Biol*, 16(2):e1007482, 2020. ISSN 1553-7358 (Electronic) 1553-734X (Linking). doi: 10.1371/journal.pcbi.1007482. URL `https://www.ncbi.nlm.nih.gov/pubmed/32017770`.

[27] Sureshnee Pillay, Jennifer Giandhari, Houriiyah Tegally, Eduan Wilkinson, Benjamin Chimukangara, Richard Lessells, Stacey Mattison, Yunus Moosa, Inbal Gazy, Maryam Fish, et al. Whole genome sequencing of sars-cov-2: Adapting illumina protocols for quick and accurate outbreak investigation during a pandemic. *bioRxiv*, 2020.

[28] Sara Cleemput, Wim Dumon, Vagner Fonseca, Wasim Abdool Karim, Marta Giovanetti, Luiz Carlos Alcantara, Koen Deforche, and Tulio De Oliveira. Genome detective coronavirus typing tool for rapid identification and characterization of novel coronavirus genomes. *Bioinformatics*, 36(11): 3552–3555, 2020.

[29] Kazutaka Katoh, Kazuharu Misawa, Kei-ichi Kuma, and Takashi Miyata. Mafft: a novel method for rapid multiple sequence alignment based on fast fourier transform. *Nucleic acids research*, 30 (14):3059–3066, 2002.

[30] A. Sigal, R. Milo, A. Cohen, N. Geva-Zatorsky, Y. Klein, I. Alaluf, N. Swerdlin, N. Perzov, T. Danon, Y. Liron, T. Raveh, A. E. Carpenter, G. Lahav, and U. Alon. Dynamic proteomics in individual human cells uncovers widespread cell-cycle dependence of nuclear proteins. *Nat Methods*, 3(7):525–31, 2006. ISSN 1548-7091 (Print) 1548-7091 (Linking). doi: 10.1038/nmeth892. URL `https://www.ncbi.nlm.nih.gov/pubmed/16791210`.

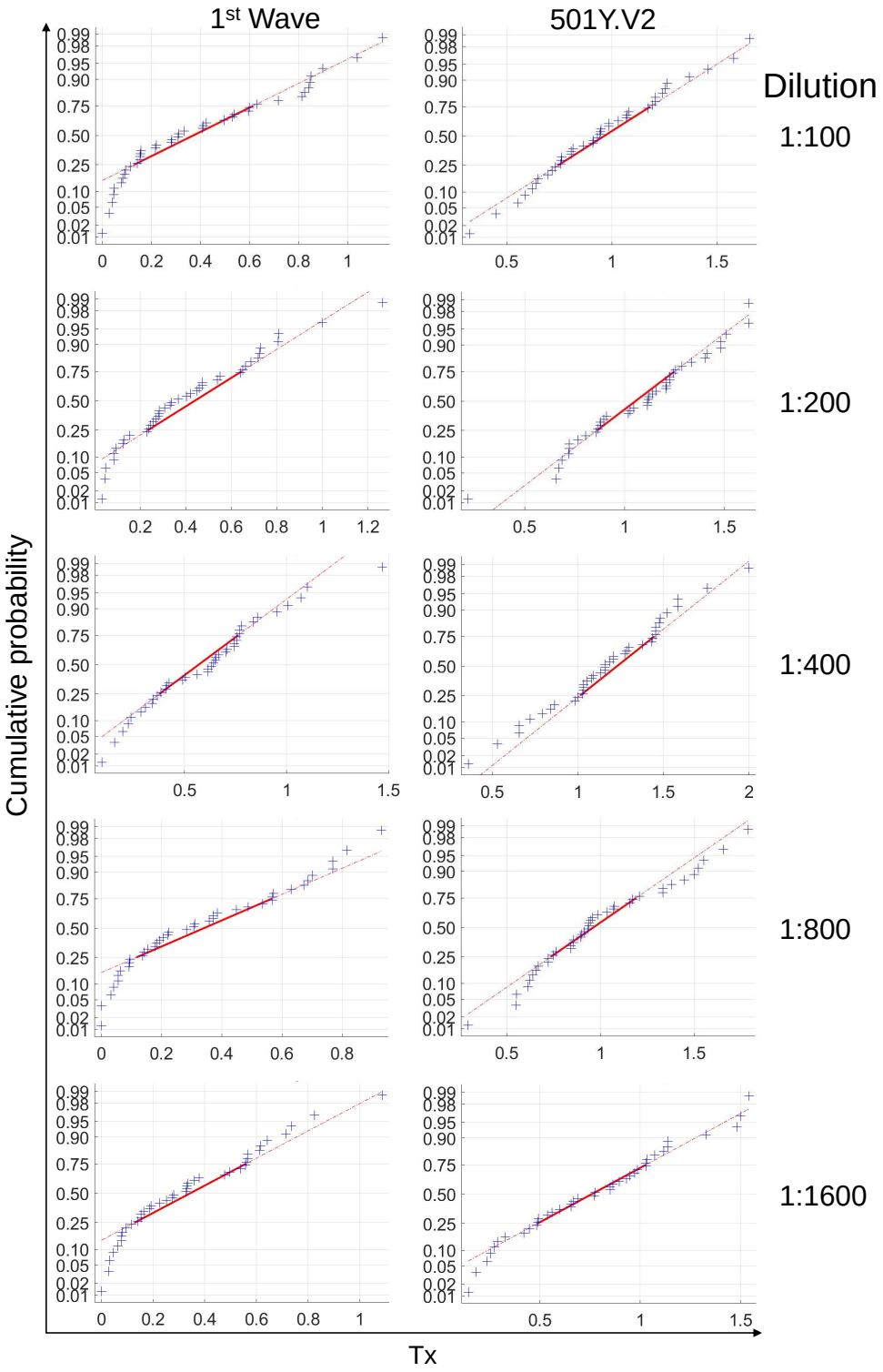

Figure S 1: Fit of combined data for each plasma dilution to a normal distribution. The Matlab2019b function normplot was used to assess the fit of the data (blue crosses) to a normal distribution (solid red line). Lack of pronounced curvature of the data in the range of the solid line indicates that a the data is a reasonably good fit to a normal distribution. see https://www.mathworks.com/help/stats/normplot.html for additional information.

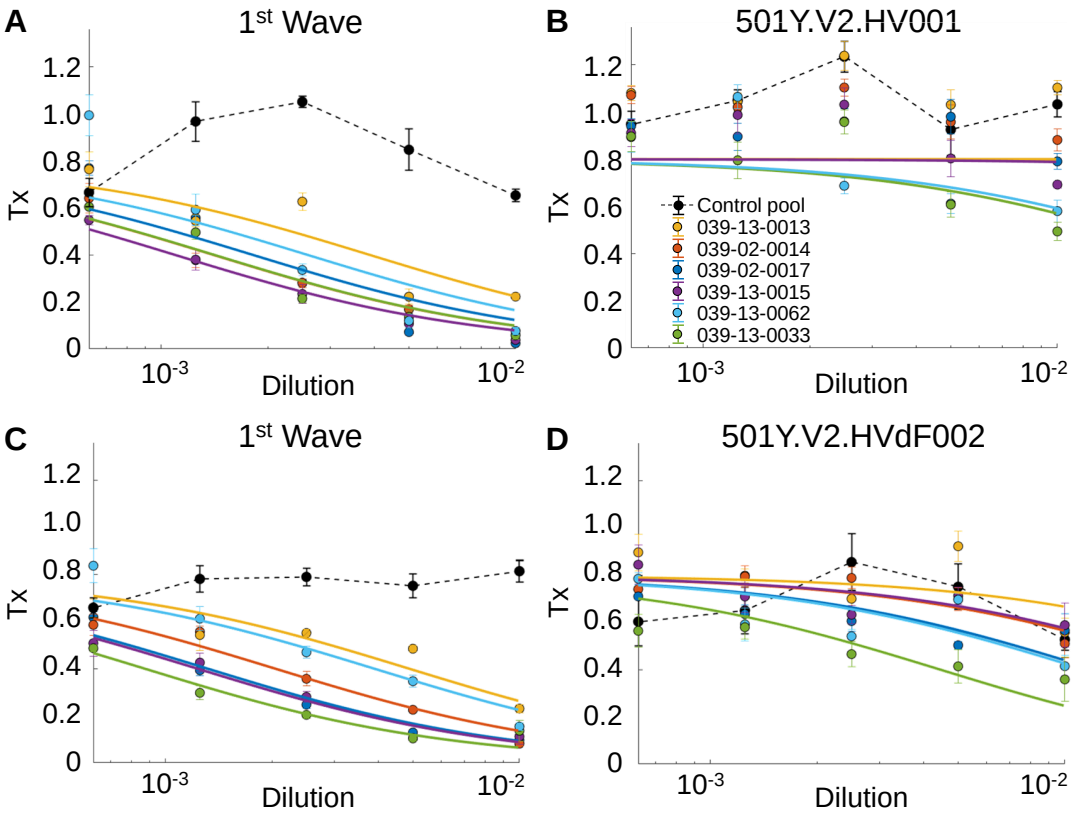

Figure S 2: Neutralization of first wave and 501Y.V2 by convalescent plasma from first wave infections separated by variant. Four sets of independent experiments were performed per 501Y.V2 - first wave pair, where the matched first wave variant results are shown to the left of the 501Y.V2 neutralization results. 501Y.V2 variant 2 contained the L18F mutation in addition to the mutations of variant 1 , and did not have the furin cleavage site deletion from outgrowth in Vero E6 cells. Colored points represent means and standard errors from 4 independent experiments for each 501Y.V2 variant/first wave pair of neutralization activity of plasma from 6 convalescent participants infected by first wave viruses. Corresponding lines are fits of the sigmoidal equation with IC_{50} as the fitted parameter. Black points represent a pool of plasma from three uninfected controls. The transmission index (Tx) is the number of foci in the presence of the plasma dilution normalized by the number of foci in the absence of plasma.

Table S 1: Plasma donor characteristics

Cohort ID	Sex	Age	Supplemental oxygen	Date of symptom onset	Days between symptom onset and diagnostic swab	Days between symptom onset and plasma collection
039-02-0014	F	66	No	01-Jul-2020	13	27
039-02-0017	F	66	Yes	21-Jul-2020	7	28
039-13-0013	F	54	No	29-Jun-2020	3	30
039-13-0015	F	42	No	21-Jun-2020	12	26
039-13-0033	F	37	No	24-Jun-2020	23	30
039-13-0062	M	67	No	06-Aug-2020	12	26

Table S 2: Mutation profile for the genomes of the outgrown viruses and for the infecting viruses of convalescent plasma donors

	Outgrown virus			Infecting virus from plasma donors					
Lineage	B.1.1	B.1.351 (510Y.V2)	B.1.351 (501Y.V2)	B.1.1	B.1.1	B.1.5	B.1.5	B.1.140	B.1.1.1
Sequence ID Accession ID Cohort ID	K002868 EPI_ISL_602622 039-13-0013	K005321 EPI_ISL_678570 -	K005325 EPI_ISL_678615 -	K002868 EPI_ISL_602622 039-13-0013	K004289 EPI_ISL_660170 039-02-0014	K004285 EPI_ISL_660167 039-13-0015	K004291 EPI_ISL_660172 039-13-0033	K004295 EPI_ISL_660167 039-02-0017	K004302 EPI_ISL_660181 039-13-0062
Spike amino acid substitutions	S:D614G S:A688V	S:D80A S:D215G S:K417N S:E484K S:N501Y S:D614G S:A701V	S:L18F S:D80A S:D215G S:K417N S:E484K S:N501Y S:D614G S:A701V	S:D614G S:A688V	S:D614G	S:D614G	S:D614G	S:D614G	S:D614G
Spike deletions		S:242-244del	S:242-244del						
Other amino acid substitutions	N:L139F N:R203K N:G204R ORF14:G50N ORF1a:D1481N ORF1b:P314L	E:P71L N:T205I ORF14:L52F ORF1a:T265I ORF1a:K1655N ORF1a:K3353R ORF1b:P314L ORF3a:Q57H ORF3a:S171L	E:P71L N:T205I ORF14:L52F ORF1a:T265I ORF1a:K1655N ORF1a:K3353R ORF1b:P314L ORF3a:Q57H ORF3a:W131L ORF3a:S171L ORF7a:V93F	N:L139F N:R203K N:G204R ORF14:G50N ORF1a:D1481N ORF1b:P314L	E:L73P N:R203K N:G204R ORF14:G50N ORF1b:P314L ORF1b:T1522I	E:L73P ORF1a:D3728N ORF1b:P314L	N:T148A ORF10:A28V ORF1a:K2511R ORF1a:V3858I ORF1b:P314L	ORF1a:F1178S ORF1b:P314L	N:R203K N:G204R ORF14:G50N ORF1a:T1246I ORF1a:G3278S ORF1b:P314L
Other deletions		orf1ab:3675-3677del	orf1ab:3675-3677del						

Lineage classification was performed by Pangolin software application version v2.1.7 (https://cov-lineages.org/pangolin.html).
Accession ID refers to GISAID EpiCoV™ database (www.gisaid.org)
Amino acid mutation nomenclature includes open reading frame, wild-type amino acid, ORF position and amino-acid mutation (e.g. S:D80A, Spike D to A substitution at position 80). del refers to deletion between stated positions. Amino acid mutations are annotated based on mature protein region of coding sequence (CDS) of SARS-CoV-2 reference sequence NC_045512.2.

Table S 3: Mutation profile for the genomes of the outgrown 501Y.V2 viruses, showing the original genome produced from the nasopharyngeal swab specimen and the genomes generated following passage in VeroE6 cells

	Outgrown 501Y.V2 Original	**Outgrown 501Y.V2 After passage 2**	**Outgrown 501Y.V2 After passage 3**	**Outgrown 501Y.V2 Original**	**Outgrown 501Y.V2 After passage 3**
Sequence ID	K005321	K007776	K007624	K005325	K007621
Spike amino acid substitutions	S:D80A S:D215G S:K417N S:E484K S:N501Y S:D614G S:A701V	S:D80A S:D215G S:K417N S:E484K S:N501Y S:D614G S:A701V	S:D80A S:D215G S:K417N S:E484K S:N501Y S:D614G S:A701V	S:L18F S:D80A S:D215G S:K417N S:E484K S:N501Y S:D614G S:A701V	S:L18F S:D80A S:D215G S:K417N S:E484K S:N501Y S:D614G S:A701V
Spike deletions	S:242-244del	S:242-244del **S:677-681del**	S:242-244del **S:677-681del**	S:242-244del	S:242-244del
Other amino acid substitutions	E:P71L N:T205I ORF14:L52F ORF1a:T265I ORF1a:K1655N ORF1a:K3353R ORF1b:P314L ORF3a:Q57H ORF3a:S171L	E:P71L N:T205I ORF14:L52F ORF1a:T265I ORF1a:K1655N ORF1a:K3353R **ORF1a:Q3878R** ORF1b:P314L ORF3a:Q57H ORF3a:S171L	E:P71L N:T205I ORF14:L52F ORF1a:T265I ORF1a:K1655N ORF1a:K3353R **ORF1a:Q3878R** ORF1b:P314L ORF3a:Q57H ORF3a:S171L	E:P71L N:T205I ORF14:L52F ORF1a:T265I ORF1a:K1655N ORF1a:K3353R ORF1b:P314L ORF3a:Q57H ORF3a:W131L ORF3a:S171L ORF7a:V93F	E:P71L **N:R32H** N:T205I ORF14:L52F ORF1a:T265I ORF1a:K1655N ORF1a:K3353R **ORF1a:N4358K** ORF1b:P314L ORF3a:Q57H ORF3a:W131L ORF3a:S171L ORF7a:V93F **ORF9b:A29T**
Other deletions	orf1ab:3675-3677del	orf1ab:3675-3677del	orf1ab:3675-3677del	orf1ab:3675-3677del	orf1ab:3675-3677del

Amino acid mutation nomenclature includes open reading frame, wild-type amino acid, ORF position and amino-acid mutation (e.g. S:D80A, Spike D to A substitution at position 80). del refers to deletion between stated positions. Amino acid mutations are annotated based on mature protein region of coding sequence (CDS) of SARS-CoV-2 reference sequence NC_045512.2. Substitutions and deletions in bold are those emerging during passage